

## Direct transition of a HfGeTe<sub>4</sub> ternary transition-metal chalcogenide monolayer with a zigzag van der Waals gap

Yuta Saito<sup>1,2\*</sup> and John Robertson<sup>2\*\*</sup>

1 Nanoelectronics Research Institute, National Institute of Advanced Industrial Science and Technology, Tsukuba Central 5, Higashi 1-1-1, Tsukuba 305-8565, Japan

2 Department of Engineering, Cambridge University, 9 J J Thomson Avenue, Cambridge CB3 0FA, United Kingdom

E-mail: \*yuta-saito@aist.go.jp, \*ys478@cam.ac.uk, \*\*jr214@cam.ac.uk

### Abstract

The ternary transition-metal chalcogenide HfGeTe<sub>4</sub> is found to have a direct band gap of around 1.3 eV in its monolayer form, while it has an indirect band gap of about a half that value in the bulk form. Contrary to the two-dimensional flat layers seen in most van der Waals solids, HfGeTe<sub>4</sub> has zigzag shaped layers. This more general shape of layers opens up a wider range of layered structures for consideration. The zigzag shape may increase adhesion between layers and provide properties useful for electrodes or insulators due to a larger surface area. The discovery of this novel transition metal ternary chalcogenide will open new avenue of materials exploration for future ultrathin electronics application.

Two-dimensional materials having a van der Waals (vdW) gap have attracted considerable attention for future electronics and optoelectronics applications since the discovery and experimental realization of graphene followed by boron nitride, black phosphorus, and transition metal dichalcogenides (TMDs).<sup>1</sup> Especially, TMDs with the chemical composition  $\text{MX}_2$  ( $\text{M}=\text{Mo}, \text{W}$  etc.,  $\text{X}=\text{S}, \text{Se}, \text{Te}$ ) possess a band gap around 1 to 2 eV, which does not exist in graphene, covering from the infra-red to visible light range, and this makes them attractive for optoelectronics and photonics applications. A typical feature of TMDs is a two-dimensional layered nature of its crystal structure, where atoms are forming strong covalent bonds within the layer, while weak van der Waals (vdW) interaction between layers. Due to this, they are easily cleaved or exfoliated even down to the monolayer (ML) limit (a few angstrom).

One of the most intriguing properties of standard  $d^2$  TMDs is that they demonstrate a direct transition when it becomes an ML, while it possesses an indirect band gap in bulk, making them promising for ultra-thin optoelectronics application as well as field effect transistor application as a high mobility channel layer.<sup>2,3</sup> However, materials exploration of TMDs is limited to just a replacement of M to different transition metals or X to chalcogen elements, which may restrict further development of such layered materials from the viewpoint of the application, where many properties are required. Recently, the transition metal trichalcogenides (TMTCs), referred to as  $\text{MX}_3$ ,<sup>4-10</sup> and the ternary transition-metal chalcogenides (TTMCs) such as  $\text{CrSiTe}_3$ ,  $\text{CrGeTe}_3$  ( $\text{Cr}_2\text{Ge}_2\text{Te}_6$ ), and  $\text{NbRhTe}_4$ ,<sup>11-14</sup> have attracted attention as a new type of layered compound. However, most  $\text{MX}_3$  studies have focused on their structural and vibrational properties except for  $\text{TiS}_3$ ,<sup>6</sup> demonstrating a new class of direct band gap material. Furthermore, magnetic or topological insulating properties are the main focus in ternary transition-metal chalcogenides. However, the indirect-direct transition, one of the most remarkable properties in TMDs and crucial for optoelectronics applications, has not been reported to date in monolayer TTMCs. The discovery of such a property would be extremely useful for applications as there significantly more ternary compounds than binary compounds, allowing a much wider range of materials to consider. Therefore, the motivation of this work is overcoming the current limitation of layered compounds and opening up the possibility of ternary compounds with an indirect-direct transition. In fact, some recent papers have reported a data mining approach on a materials database combined with density functional theory (DFT) simulations in order to efficiently

search for novel unknown two-dimensional materials.<sup>15-18</sup>

Here we propose HfGeTe<sub>4</sub> as a novel layered material.<sup>19-22</sup> Less is known about this material and no electronic structure has been reported in its ML structure. It should be noted that even though screening methods using DFT is a powerful tool, this compound has been overlooked to date in any papers.<sup>15-18</sup> Therefore, proving the possibility of this material as a new layered compound is particularly important. If one treats Hf and Ge as a cation atom, HfGeTe<sub>4</sub> can be represented as M<sub>2</sub>Te<sub>4</sub> (M=Hf, Ge), or MTe<sub>2</sub>, as in a conventional TMD, MX<sub>2</sub>. Therefore, by analogy, an indirect to direct transition could be expected at the ML limit. The distinctive difference of this material to other TMDs is the zigzag vdW gap as shown in Figure 1.<sup>19</sup> One of the challenging issues of TMDs in terms of integration for practical application in industry can be its atomically-flat passivated surface that may result in poor adhesion between an electrode or other surrounding materials because of the weak interaction. In fact, delamination of a metal electrode film from an atomically-flat molecular beam epitaxy (MBE) grown layered Sb<sub>2</sub>Te<sub>3</sub> film has been reported recently,<sup>23</sup> suggesting poor adhesion that may inhibit applications of such materials. Since the zigzag surface has a significantly larger surface area than flat one, an improvement of adhesion strength could be expected. In this paper, the electronic band structure of bulk and monolayer HfGeTe<sub>4</sub> is compared. We theoretically demonstrate the direct evidence of the indirect-direct transition of the band structure in the monolayer HfGeTe<sub>4</sub>.

A CASTEP code was used with norm conserving pseudopotentials.<sup>24</sup> For geometry optimization, the generalized gradient approximation (GGA) of Perdew-Burke-Ernzerhof (PBE) was used,<sup>25</sup> and plane wave cutoff energy was 440 eV. A 2×2×1 and 6×6×2 Monkhorst-Pack k-point mesh were used for geometry optimization for monolayer and bulk, respectively.<sup>26</sup> For monolayer calculations, 20 Å of a vacuum slab was inserted in order to avoid the interaction between layers. The model structures were relaxed until the residual force is below 0.03 eV/Å. Van de Waals interaction were included using a DFT-D correction term.<sup>27</sup> A 3×1×1 k-point mesh was used to calculate the density of states (DOS). The screened exchange (sX) hybrid functional was used for DOS and band structure calculations in order to correct the band gap underestimation in GGA.<sup>28</sup>

The crystal structure of bulk HfGeTe<sub>4</sub> is shown in Fig. 1(a). It is orthorhombic with the space group No. 36 (*Cmc*2<sub>1</sub>) and lattice constants are  $a = 3.963\text{\AA}$ ,  $b = 10.941\text{\AA}$ , and  $c =$

15.875Å.<sup>19</sup> The unit cell drawn by blue lines includes two layers. As shown in Fig. 1(b), the inter layer distances vary between 3.6 to 4.3 Å depending on the choice of two atoms and these relatively large values clearly indicate the vdW-type weak interaction. Fig. 1(c) schematically demonstrates the crystal structure from the x-axis to highlight a zigzag nature of the vdW gap. This zigzag gap is a notable difference with the typical two-dimensional flat TMDs, and is expected to show better adhesion strength with surrounding materials due to its larger surface area. A monolayer of HfGeTe<sub>4</sub> is shown in Fig. 1(d), where Hf atoms have eight-coordination with seven Te atoms and one Ge atom, and Ge atoms are tetrahedrally coordinated with three Te and one Hf. If one sees this structure from the front to the back of the paper, one dimensional (1D) chain-like structures with trigonal prisms can be recognized. The layered materials having such the 1D chain has been recently referred to pseudo-1D or quasi-1D materials (MS<sub>3</sub>; M=Ti, Zr, and Hf) and have been intensively studied as a new type of layered materials with anisotropic properties.<sup>5,7-10</sup> The appearances of the crystal structure from different directions are summarized in Fig. 1(e).

Figures 2(a) and (b) represent a unit cell of monolayer and a corresponding schematic reciprocal lattice, respectively, where representative high symmetry points are depicted. The calculated band structures of bulk and ML HfGeTe<sub>4</sub> are shown in Fig. 2(c) and (d). The bulk has a band gap of about 0.67 eV and a transition occurs from the  $\Gamma$  point in the valence band maximum (VBM) to the Y point in the conduction band minimum (CBM), indicating an indirect semiconductor. On the other hand, the direct transition is realized at the  $\Gamma$  point in ML with the band gap of 1.3 eV. This is exactly the same trend observed in typical TMDs. The VBM is identical in the bulk and ML and is at the  $\Gamma$  point, whereas the CBM at the Y point in bulk goes higher energy in ML, which results in the CBM being at the  $\Gamma$  point. One of the possible origins of the indirect-direct transition observed may be due to the zigzag nature of the crystal structure along y-axis. The direction from  $\Gamma$  to Y corresponds to the zigzag direction (Fig. 1(e), Fig. 2(a), (b)). As can be seen in Fig. 1(b), the top atom in the one zigzag layer and the bottom atom in the above layer are overlapping each other along the y direction. Therefore, the disappearance of interaction with neighboring layers in ML will significantly affect the band dispersion along this direction. This hypothesis anticipates that adding number of layers may change the band dispersion around the Y point.

Figure 3(a) shows the calculated band gaps as a function of the number of layers. It

was found that only the ML exhibited the direct transition and models more than 2ML show the indirect transition, demonstrating the same trend with TMDs. The full set of band structures as a function of thickness is summarized in Supporting Figure 1. Moreover, the band gap decreases with increasing the number of layer toward the bulk limit. This is also a general trend of TMDs. The inset shows the  $\log(E_g - E_B)$  vs.  $\log N$  plot based on a well-known power law,  $E_g = E_B + A/N^n$ , where  $E_g$  is the band gap of a given structure,  $E_B$  is the band gap of bulk,  $N$  is the number of layers, and  $A$  and  $n$  are fitting parameters.<sup>29,30</sup> Note that 2, 3, and 4ML results were used to get a fitting and ML is not considered due to the lack of layer interactions. According to this trend, the strongest photoluminescence (PL) intensity will be expected in the ML film of HfGeTe<sub>4</sub> and the intensity will be exponentially decreased with the thickness accompanying with the red shift of the peak position. The detailed band dispersions around the Y point as a function of the number of layers are summarized in Fig. 3(b). In order to clarify the figure, only the curves of the VBM and CBM for each model are drawn. It can be seen that the VBM locates at the  $\Gamma$  point for all structures, while the bands around the Y point strongly depend on the thickness and increase with decreasing the thickness. Moreover, the relative energy of the CBM at the  $\Gamma$  point to the Y point strongly affected by the thickness. Namely, the band energy monotonically increases from  $\Gamma$  to Y in ML, while it has a minimum value at the Y point when thickness becomes more than two layers. These results support the above discussed hypothesis that the interactions between interlayers are playing a crucial role, which determines the electronic band structures, especially the type of transition. It should be noted that different pseudopotentials give slightly different results as shown in Supporting Fig. 2. In the case of the ultrasoft pseudopotential, the energy of conduction band at the Y point is relatively lower than that of obtained by the norm conserving pseudopotential although both results still demonstrate the direct transition. Therefore, it can be speculated that the dispersion of conduction band is sensitive to the calculation conditions. Regardless of such variations, we believe that the HfGeTe<sub>4</sub> has nearly a direct band gap in the ML form due to less interlayer interaction for bendy layers, and that further detailed calculations as well as experimental confirmation would be necessary.

The total DOS and partial (P)DOS of bulk and ML are compared in Figure 4. It was found that the overall DOS features in the bulk and ML are very similar. The VBM is mainly composed of Hf-*d* and Te-*p* states, while the CBM is Hf-*d* and Ge-*p* states. The

former feature is similar to TMDs, such as MoS<sub>2</sub>,<sup>31</sup> where the VBM and CBM consist of Mo-*d* and S-*p* states. On the other hand, Te-*p* in HfGeTe<sub>4</sub> is very weak at the CBM inconsistent with TMDs, whereas Ge-*p* states instead are contributing to the CBM in addition to Hf-*d*. This may be explained by the previous work reporting that Ge can be viewed as behaving as a cation when it coordinates with Te and also as an anion for its bonds to Hf atoms.<sup>19</sup> This is a clear difference from MoS<sub>2</sub> where only the metal-chalcogen bonding exists, but the Hf-Ge bond exists in HfGeTe<sub>4</sub>. Such the anionic feature of Ge may contribute to the formation of the CBM instead of Te. The PDOS of Ge seems like typical *sp*<sup>3</sup> type feature, where the *s*-state is localized in the relatively deeper level and *p*-states make bonding and anti-bonding states at near the VBM and in the conduction band, respectively. This could be attributed to that Ge holds the tetrahedral coordination in HfGeTe<sub>4</sub> as shown in Fig. 1.

Finally, we compare the band alignments of the HfGeTe<sub>4</sub> ML with bulk. Fig. 5 shows the valence and conduction bands of HfGeTe<sub>4</sub>. The results of other TMDs are also shown for comparison.<sup>32</sup> The general trend is very similar in HfGeTe<sub>4</sub> and TMDs that the band gap is larger in ML than bulk, and the shift of the energy in the VBM is greater than CBM. These results suggest that HfGeTe<sub>4</sub> possesses very similar properties with TMDs in terms of the electronic structure, especially in the monolayer limit.

Because of more complicated zigzag structure of HfGeTe<sub>4</sub> that clearly distinguishes it from the simple atomically-flat TMDs, mechanical exfoliation seems more challenging. On the other hand, a bottom-up process, such as chemical vapor deposition (CVD) or physical vapor deposition (PVD), which have more advantage for industry, may enable to grow this material. Once it is successfully formed, the adhesion strength with metal or insulator layers would be stronger than the flat structure. Experimental realization of the synthesis of this material and measurements of optoelectronic properties as well as adhesion strength will be expected in future. Moreover, recently, not only two-dimensional materials itself but also the vdW-heterostructures as well as chalcogenide superlattice consisting of at least two different layered materials have been paying attention because of emergence of multi-functional features.<sup>33-35</sup> Therefore, it is expected that HfGeTe<sub>4</sub> would be also an interesting material as a component of such heterostructure.

In conclusion, we theoretically predict the indirect to direct transition of the monolayer HfGeTe<sub>4</sub> ternary transition-metal chalcogenide (TTMC). Surprisingly we have observed

several resemblances to typical transition metal dichalcogenides (TMDs), MoS<sub>2</sub>, for example, the direct transition only in ML, band gap decrement with the thickness, and the band alignment. On the other hand, more elements in HfGeTe<sub>4</sub> than MoS<sub>2</sub> make the crystal structure more complicated resulting in the zigzag shaped van der Waals gap. This would be expected to enhance the adhesion property with surrounding materials that is crucial for application of the layered materials in the real industry. Based on the current study, the materials exploration of layered chalcogenides will dramatically extend from binary to ternary systems that may lead discovery of novel materials for future electronics applications.

#### Acknowledgements

We acknowledge EPSRC/JPPS core to core grant.

#### References

- <sup>1</sup> A. K. Geim and I. V. Grigorieva, “Van der Waals heterostructures”, *Nature* **499**, 419 (2013).
- <sup>2</sup> K. F. Mak, C. Lee, J. Hone, J. Shan, and T. F. Heinz, “Atomically thin MoS<sub>2</sub>: A new direct-gap semiconductor”, *Phys. Rev. Lett.* **105**, 136805 (2010).
- <sup>3</sup> B. Radisavljevic, A. Radenovic, J. Brivio, V. Giacometti, and A. Kis, “Single-layer MoS<sub>2</sub> transistors”, *Nat. Nanotech.* **6**, 147 (2011).
- <sup>4</sup> M. Li, J. Dai, and X. C. Zeng, “Tuning the electronic properties of transition-metal trichalcogenides via tensile strain”, *Nanoscale* **7**, 15385 (2015).
- <sup>5</sup> A. Lipatov, P. M. Wilson, M. Shekhirev, J. D. Teeter, R. Netusil, and A. Sinitskii, “Few-layered titanium trisulfide (TiS<sub>3</sub>) field-effect transistors”, *Nanoscale* **7**, 12291 (2015).
- <sup>6</sup> J. Dai and X. C. Zeng, “Titanium trisulfide monolayer: Theoretical prediction of a new direct-gap semiconductor with high and anisotropic carrier mobility”, *Angew. Chem. Int. Edit.* **54**, 7572 (2015).
- <sup>7</sup> J. O. Island, R. Biele, M. Barawi, J. Clamagirand, J. Ares, C. S´anchez, H. S. J. van der Zant, I. J. Ferrer, R. D’Agosta, and A. Castellanos-Gomez, “Titanium trisulfide (TiS<sub>3</sub>): a 2D semiconductor with quasi-1D optical and electronic properties”, *Sci. Rep.* **6**, 22214 (2016).
- <sup>8</sup> A. Pant, E. Torun, B. Chen, S. Bhat, X. Fan, K. Wu, D. P. Wright, F. M. Peeters, E.

Soignard, H. Sahin, and S. Tongay, “Strong dichroic emission in the pseudo one dimensional material ZrS<sub>3</sub>”, *Nanoscale* **8**, 16259 (2016).

<sup>9</sup> K. Wu, E. Torun, H. Sahin, B. Chen, X. Fan, A. Pant, D. Parsons Wright, T. Aoki, F. M. Peeters, E. Soignard, and S. Tongay, “Unusual lattice vibration characteristics in whiskers of the pseudo-one- dimensional titanium trisulfide TiS<sub>3</sub>”, *Nat. Commun.* **7**, 12952 (2016).

<sup>10</sup> W. Kong, C. Bacaksiz, B. Chen, K. Wu, M. Blei, X. Fan, Y. Shen, H. Sahin, D. Wright, D. S. Narang, and S. Tongay, “Angle resolved vibrational properties of anisotropic transition metal trichalcogenide nanosheets”, *Nanoscale* **9**, 4175 (2017).

<sup>11</sup> N. Sivadas, M. W. Daniels, R. H. Swendsen, S. Okamoto, and D. Xiao, “Magnetic ground state of semiconducting transition-metal trichalcogenide monolayers”, *Phys. Rev. B* **91**, 235425 (2015).

<sup>12</sup> J. Liu, H. Wang, C. Fang, L. Fu, and X. Qian, “Van der Waals stacking-induced topological phase transition in layered ternary transition metal chalcogenides”, *Nano Lett.* **17**, 467 (2017).

<sup>13</sup> C. Gong, L. Li, Z. Li, H. Ji, A. Stern, Y. Xia, T. Cao, W. Bao, C. Wang, Y. Wang, Z. Q. Qiu, R. J. Cava, S. G. Louie, J. Xia, and X. Zhang, “Discovery of intrinsic ferromagnetism in two-dimensional van der Waals crystals”, *Nature*, **546**, 265 (2017).

<sup>14</sup> S. Hatayama, Y. Sutou, S. Shindo, Y. Saito, Y.-H. Song, D. Ando, and J. Koike, “Inverse Resistance Change Cr<sub>2</sub>Ge<sub>2</sub>Te<sub>6</sub>-Based PCRAM Enabling Ultralow-Energy Amorphization”, *ACS Appl. Mater. Interfaces*, DOI: 10.1021/acsami.7b16755 (2017).

<sup>15</sup> S. Lebègue, T. Björkman, M. Klintonberg, R. M. Nieminen, and O. Eriksson, “Two-dimensional materials from data filtering and ab initio calculations”, *Phys. Rev. X*, **3**, 031002 (2013).

<sup>16</sup> M. Nicolas, G. Marco, S. Philippe, M. Andrius, C. Ivano E., C. Andrea, P. Giovanni, and M. Nicola, “Novel two-dimensional materials from high-throughput computational exfoliation of experimentally known compounds”, arXiv:1611.05234, (2016).

<sup>17</sup> G. Cheon, K.-A. N. Duerloo, A. D. Sendek, C. Porter, Y. Chen, and E. J. Reed, “Data mining for new two- and one-dimensional weakly bonded solids and lattice-commensurate heterostructures”, *Nano Lett.* **17**, 1915 (2017).

<sup>18</sup> K. Choudhary, I. Kalish, R. Beams, and F. Tavazza, “High-throughput identification and characterization of two-dimensional materials using density functional theory”, *Sci. Rep.* **7**, 5179 (2017).



- <sup>19</sup> A. Mar and J. A. Ibers, “The layered ternary germanium tellurides  $ZrGeTe_4$ ,  $HfGeTe_4$ , and  $TiGeTe_6$ : structure, bonding, and physical properties”, *J. Am. Chem. Soc.* **115**, 3227 (1993).
- <sup>20</sup> G.-J. Jang and H. Yun, “Hafnium germanium telluride”, *Acta Cryst. E* **64**, i27 (2008).
- <sup>21</sup> R. Sheeba, S. Israel, and S. Saravanakumar, “Investigation of the van der Waals epitaxy gap in isostructural semiconducting germanium tellurides:  $HfGeTe_4$  and  $ZrGeTe_4$ ”, *Chi. J. Phys.* **54**, 668 (2016).
- <sup>22</sup> Y. Saito, Y. Sutou, P. Fons, S. Shindo, X. Kozina, J. M. Skelton, A. V. Kolobov, and K. Kobayashi, “Electronic structure of transition-metal based  $Cu_2GeTe_3$  phase change material: Revealing the key role of Cu *d* electrons”, *Chem. Mater.* **29**, 7440 (2017).
- <sup>23</sup> J. E. Boschker, E. Tisbi, E. Placidi, J. Momand, A. Redaelli, B. J. Kooi, F. Arciprete, and R. Calarco, “Textured  $Sb_2Te_3$  films and  $GeTe/Sb_2Te_3$  superlattices grown on amorphous substrates by molecular beam epitaxy”, *AIP Adv.* **7**, 015106 (2017).
- <sup>24</sup> S. J. Clark, M. D. Segall, C. J. Pickard, P. J. Hasnip, M. I. J. Probert, K. Refson, and M. C. Payne, “First principles methods using CASTEP”, *Z. Kristallogr.* **220**, 567 (2005).
- <sup>25</sup> J. P. Perdew, K. Burke, and M. Ernzerhof, “Generalized gradient approximation made simple”, *Phys. Rev. Lett.* **77**, 3865 (1996).
- <sup>26</sup> H. J. Monkhorst and J. D. Pack, “Special points for Brillouin-zone integrations”, *Phys. Rev. B* **13**, 5188 (1976).
- <sup>27</sup> S. Grimme, J. Antony, S. Ehrlich, and H. Krieg, “A consistent and accurate ab initio parametrization of density functional dispersion correction (DFT-D) for the 94 elements H-Pu”, *J. Chem. Phys.* **132**, 154104 (2010).
- <sup>28</sup> S. J. Clark and J. Robertson, “Screened exchange density functional applied to solids”, *Phys. Rev. B* **82**, 085208 (2010).
- <sup>29</sup> H. Liu, A. T. Neal, Z. Zhu, Z. Luo, X. Xu, D. Tománek, and P. D. Ye, “Phosphorene: An unexplored 2D semiconductor with a high hole mobility” *ACS Nano* **8**, 4033 (2014).
- <sup>30</sup> Y. Guo and J. Robertson, “Vacancy and doping states in monolayer and bulk black phosphorus”, *Sci. Rep.* **5**, 14165 (2015).
- <sup>31</sup> E. S. Kadantsev and P. Hawrylak, “Electronic structure of a single  $MoS_2$  monolayer”, *Sol. State Comm.* **152**, 909 (2012).
- <sup>32</sup> Y. Guo and J. Robertson, “Band engineering in transition metal dichalcogenides: Stacked versus lateral heterostructures”, *Appl. Phys. Lett.* **108**, 233104 (2016).

<sup>33</sup> K. S. Novoselov, A. Mishchenko, A. Carvalho, and A. H. Castro Neto, “2D materials and van der Waals heterostructures”, *Science*, **353**, aac9439 (2016).

<sup>34</sup> Y. Liu, N. O. Weiss, X. Duan, H.-C. Cheng, Y. Huang, and X. Duan, “Van der Waals heterostructures and devices”, *Nat. Rev. Mater.* **1**, 16042 (2016).

<sup>35</sup> R. E. Simpson, P. Fons, A. V. Kolobov, T. Fukaya, M. Krbal, T. Yagi, and J. Tominaga, “Interfacial phase-change memory”, *Nat. Nanotech.* **6**, 501 (2011).

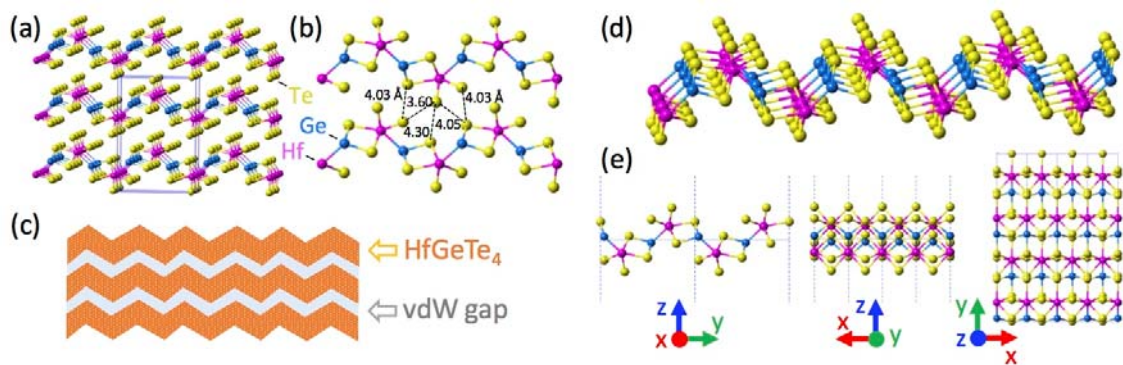


Figure 1. (a) A crystal structure of bulk HfGeTe<sub>4</sub>. The unit cell is shown as blue lines. (b) The view from x-axis to show the distances between atoms in interlayers. (c) A schematic illustration of a zigzag vdW gap. (d) An ML structure. (e) The views from x-, y-, and z-axes.

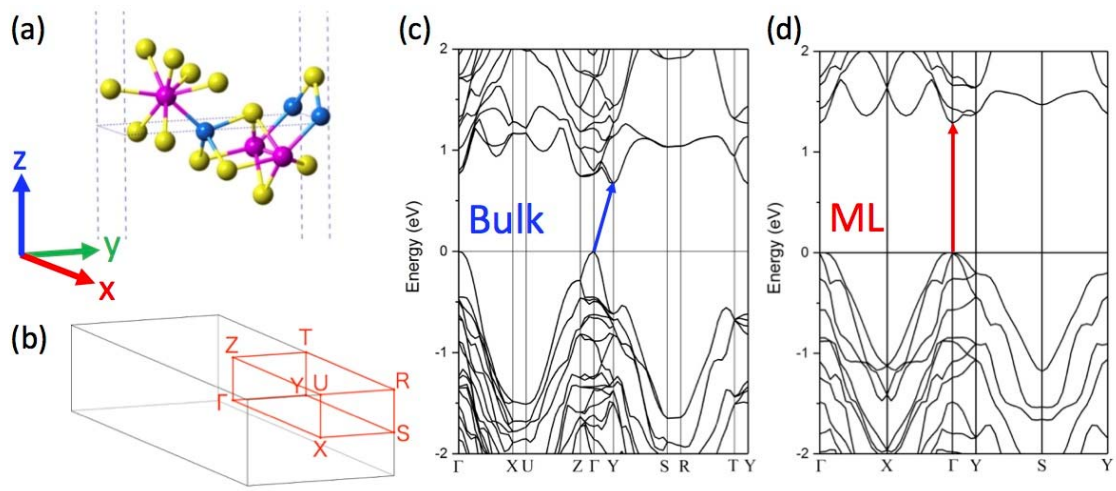


Figure 2. (a) The crystal structure of ML HfGeTe<sub>4</sub> and (b) the corresponding schematic reciprocal lattice. Calculated band structure of (c) bulk and (d) ML.

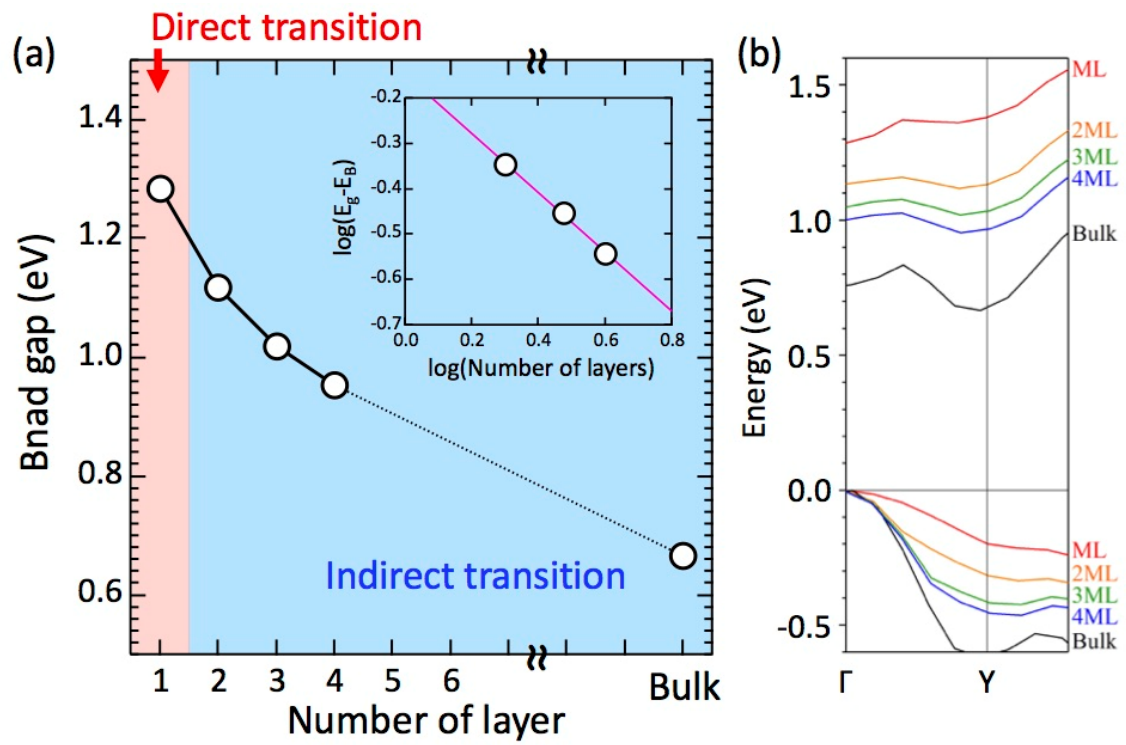


Figure 3. (a) Band gap vs number of layers. Inset shows fitting of band gap as a function of number of layers. (c) Enlarged band structures between the  $\Gamma$  and Y points as a function of number of layers.

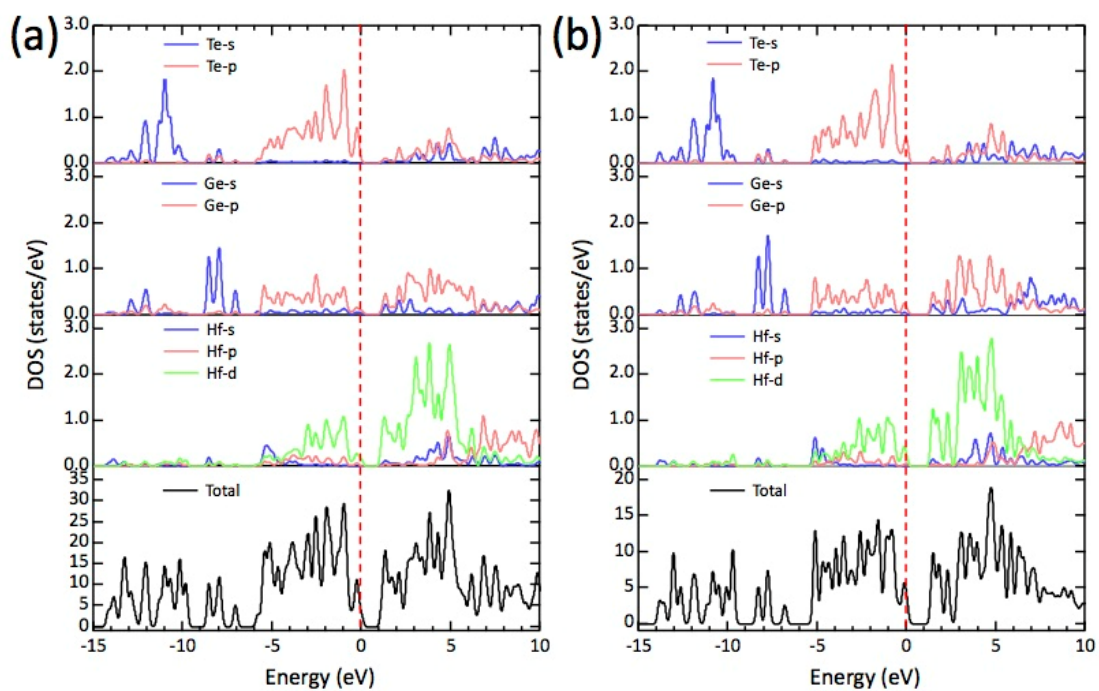


Figure 4. Calculated DOS of (a) bulk and (b) ML.

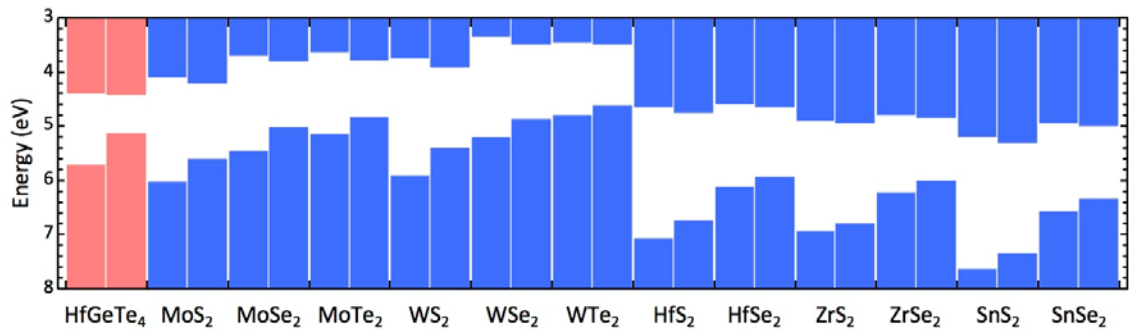
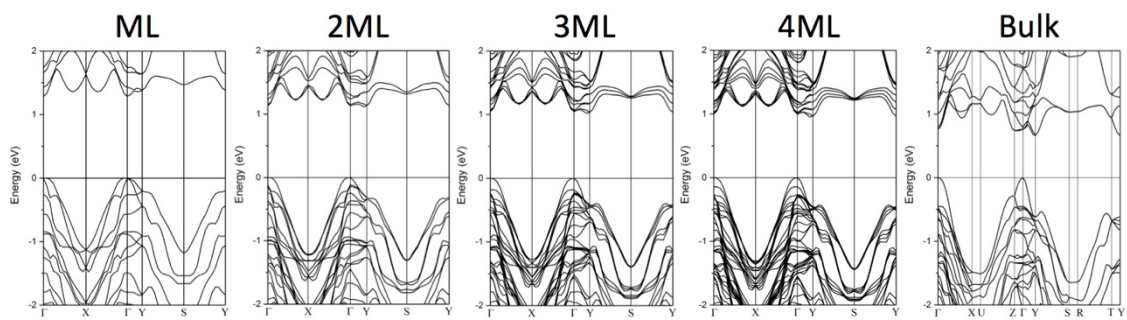
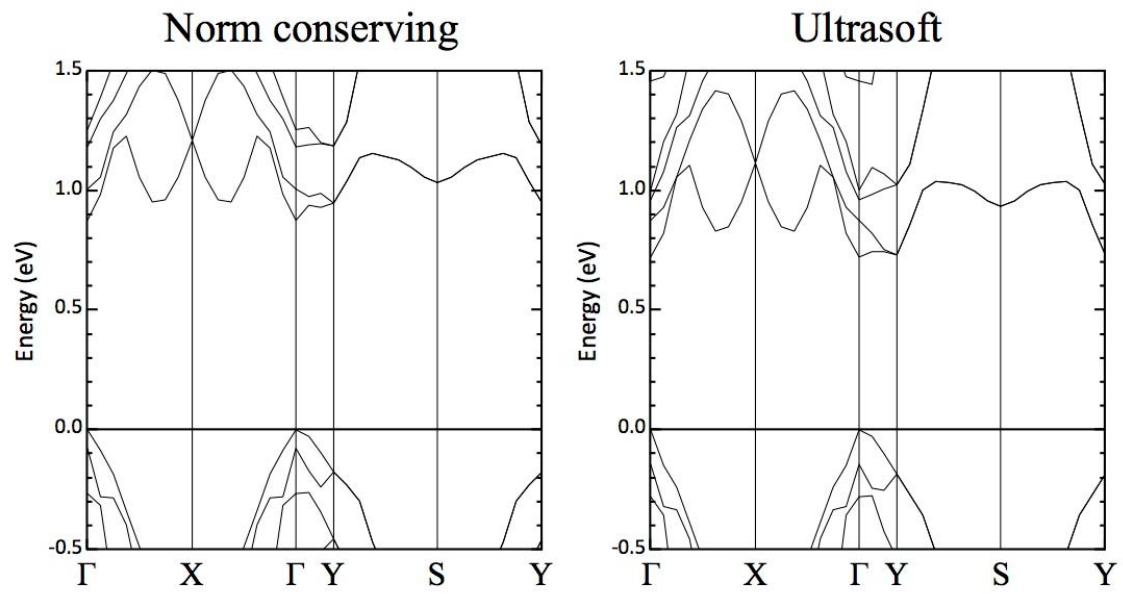


Figure 5. Band alignment of ML and bulk of HfGeTe<sub>4</sub>. The data of other TMDs are also shown for comparison.<sup>32</sup> For each compound, left is the result of monolayer and right is bulk.



Supplemental Figure 1. Band structures of HfGeTe<sub>4</sub> with different number of layers.





Supplemental Figure 2. Band structures of  $\text{HfGeTe}_4$  ML with different pseudopotentials. A GGA functional was used.